International Journal of Refrigeration 141 (2022) 66–75

Contents lists available at ScienceDirect

International Journal of Refrigeration

journal homepage: www.elsevier.com/locate/ijrefrig

Experimental evaluation of a transcritical CO_2 refrigeration facility working with an internal heat exchanger and a thermoelectric subcooler: Performance assessment and comparative

Évaluation expérimentale d'une installation frigorifique au CO2 transcritique fonctionnant avec un échangeur interne de chaleur et un sous-refroidisseur thermoélectrique : évaluation des performances et comparaison

Álvaro Casi [a], Patricia Aranguren [a], Miguel Araiz [a,*], Daniel Sanchez [b], Ramon Cabello [b], David Astrain [a]

[a] Department of Engineering, Institute of Smart Cities, Public University of Navarre, Campus de Arrosadia s/n E-31006, Pamplona, Spain
[b] Department of Mechanical Engineering and Construction, Jaume I University, Campus de Riu Sec s/n E-12071 Castellón, Spain

ARTICLE INFO

Keywords:
Transcritical cycle
Subcooling
Thermoelectric subcooler
IHX
CO_2
R744

Mots clés:
Cycle transcritique
Sous-refroidissement
Sous-refroidisseur thermoélectrique
Échangeur interne de chaleur (IHX)
CO_2
R744

ABSTRACT

The use of carbon dioxide in transcritical state has become one of the most used solutions to comply with the F-Gas directive and reduce greenhouse gases emissions from refrigeration systems at high ambient temperatures. For low-medium power units, the commonly used solutions to improve the efficiency such as the ejector, multiple compressor arrangements, mechanical subcooler, etc., add complexity and increase the cost of the refrigeration facility, which is not ideal for small units. In this low-medium power range, two technologies stand out to increase the performance of a carbon dioxide transcritical cycle: the internal heat exchanger and the thermoelectric subcooler. This study brings a complete research in which both solutions have been tested in the same experimental transcritical carbon dioxide refrigeration facility under the same working conditions. It focuses on the real performance of both systems and discusses the strengths and weaknesses of using an internal heat exchanger or a thermoelectric subcooler. The results show that the thermoelectric subcooler outperforms the internal heat exchanger in both the coefficient of performance and the cooling capacity while also being a more controllable and flexible solution.

1. Introduction

In 2019, the refrigeration sector, including air conditioning, consumed 20% of the electricity used worldwide and according to an estimate of the International Institute of Refrigeration, the electric demand of the sector could increase over a 100% by 2050 IIR (2019). The aforementioned sector is responsible for 7.8% of worldwide greenhouse gas emissions with a total of 4.14 $GtCO_2eq$ emitted to the atmosphere each year IIR (2017). The global warming impact of refrigeration systems is divided in two terms: the direct emissions related to the leakage of fluorinated refrigerants, that account for 37% of the environmental impact of a refrigeration facility, and the indirect emissions that are produced by the electrical energy consumption of the system that account for the remaining 63% IIR (2017).

In order to reduce the direct emissions, the use of carbon dioxide (CO_2) as an alternative to fluorinated fluids has become a frequent solution due to its virtually negligible global warming potential (GWP), which almost reduces the direct emissions of a refrigeration system to zero. As a result, the number of refrigeration systems that use CO_2 as a refrigerant have increased in the last years, particularly in the north of Europe, where CO_2 vapour compression cycles achieve high coefficients of performance (COP) Shecco (2016). The high efficiency of CO_2 refrigeration systems in northern countries, due to lower ambient

* Corresponding author.
E-mail address: miguel.araiz@unavarra.es (M. Araiz).

https://doi.org/10.1016/j.ijrefrig.2022.05.024
Received 11 March 2022; Received in revised form 28 April 2022; Accepted 27 May 2022
Available online 28 May 2022

Variables

c_p	Specific heat capacity at constant pressure ($Jkg^{-1}K^{-1}$)
COP	Coeficcient of performance
h	Enthalpy ($KJKg^{-1}$)
$\dot{m}$	Mass flow rate (kgh^{-1})
P	Pressure (bar)
$\dot{Q}$	Heat flux (W)
RH	Relative humidity (%)
Sub	Subcooling (K)
T	Temperature (° C)
USH	Useful superheating (K)
V	Voltage (V)
$\dot{V}$	Volumetric flow rate ($m^3\ h^- - 1$)
$\dot{W}$	Power consumption (W)
ρ	Density (Kgm^{-3})

Subscripts and superscripts

0	Evaporator
amb	Ambient
base	Base cycle
CO2	Carbon dioxide
comp	Compressor
crit	Critical
dis	Discharge
evap	Evaporation level
gc	Gas-cooler
gly	Mixture of water-glycol (40% glycol)
IHX	Internal heat exchanger
opt	Optimum working conditions
TEM	Thermoelectric module
TEMs	Thermoelectric modules
TESC	Thermoelectric subcooler
tot	Total

temperature, results in almost negligible direct emission systems with competitive power consumption and hence, similar indirect emissions than the use of fluorinated fluids.

However, in southern countries, utilising CO_2 as a working fluid for vapour compression cycles has various drawbacks that need to be technically addressed. Unlike conventional refrigerants, due to the critical temperature of CO_2 ($T_{crit\ CO2} = 30.98°C$), vapour compression systems that use CO_2 are forced to work under transcritical conditions when ambient temperature surpass a certain threshold Robinson and Groll (1998). The resulting transcritical cycle has significant exergy losses that decrease the efficiency of the refrigeration facility Kim et al. (2004). This is translated in greater energy consumption and higher indirect emissions that diminishes the competitiveness of CO_2 refrigeration systems when ambient temperature is high Cecchinato et al. (2010).

In order to decrease energy consumption and thus, reduce the indirect emissions of the CO_2 transcritical cycle, many technologies have arose over the past years to improve the efficiency of these systems. Some of the more noticeable ones are: parallel compressors Sarkar and Agrawal (2010), gas ejectors Liu et al. (2012); Zhu et al. (2017), integrated mechanical subcoolers Nebot-Andrés et al. (2020), dedicated mechanical subcoolers Dai et al. (2022) or multi-stage compressor systems Catalán-Gil et al. (2020); Chesi et al. (2014); Llopis et al. (2015). These solutions, even though they increase the performance of the refrigeration system, they involve an increase in cost and complexity of the system that are only fitted for high power refrigeration facilities. For low-medium power units, the aforementioned technologies are not appropriate. In this low-medium power range, recent studies have been directed to two practical solutions to improve the performance of transcritical CO_2 refrigeration cycles: thermoelectric subcoolers (TESC) and internal heat exchangers (IHX).

Including a TESC in a transcritical CO_2 refrigeration cycle has been the focus of recent studies due to its robustness, compactness, easy control and durability. A TESC is a novel solution that is based on the use of thermoelectric modules (TEMs), that take advantage of the Peltier effect to force a heat flux using electrical power Sharma et al. (2014). In a transcritical CO_2 refrigeration cycle, the system subcools the refrigerant at the outlet of the gas-cooler, increasing the specific cooling capacity and introducing the power consumption of the TEMs. If properly managed, the increase in cooling capacity compensates the extra consumption and the final effect results in an enhancement in both the cooling capacity and the COP of the transcritical CO_2 refrigeration cycle. Schoenfield et al. obtained an experimental improvement in the COP of 5.2% and a maximum increase in the cooling capacity of 15.3% after including a TESC Schoenfeld et al. (2008). Sanchez et al., in an experimental refrigeration test bench, reported an enhancement in the COP of 9.9% and an increase in the cooling capacity of 16% using a TESC Sánchez et al. (2020). Subsequently, Aranguren et al. performed an optimization of the voltage supplied to the TEMs of the same experimental facility, achieving an enhancement in the COP of 11.3% and an increase in the cooling capacity of 15.3% with the TESC Aranguren et al. (2021).

The use of an IHX is one of the most commonly used technologies to improve the efficiency of a transcritical CO_2 refrigeration cycle. It consists of a heat exchanger that allows a heat flux between the refrigerant at high pressure at the outlet of the gas-cooler and the low pressure refrigerant at the outlet of the evaporator. The effect of the device is an increase in specific cooling capacity and specific compression work, which can either improve or worsen the efficiency of the system depending on the refrigerant, dimensions of the IHX or working conditions. Aprea and Maiorino reported a 10% improvement in the COP using an IHX in a transcritical CO_2 cycle for air conditioning in an experimental setup Aprea and Maiorino (2008). Regarding refrigeration systems, Torrella et al. managed to experimentally obtain a maximum enhancement of 12% in both the cooling capacity and the efficiency of a transcritical CO_2 facility using an IHX Torrella et al. (2011).

The use of a TESC or an IHX present themselves as great solutions for low-medium power refrigeration applications. However, the experimental studies performed for these systems were conducted for facilities with different cooling capacity, components, or even working conditions such as: evaporation level, gas-cooler pressure, ambient temperature, useful superheating etc. To properly asses, evaluate and compare the benefits of both technologies, they have to be tested for the same facility and under the same working conditions. For that purpose, this study brings, for the first time, a complete experimental research of a novel TESC and an IHX in a transcritical CO_2 refrigeration facility that aims to compare the two technologies and evaluate their strengths and weaknesses.

In this work, an experimental transcritical CO_2 refrigeration facility has been tested with a novel TESC system and an IHX under real working conditions. Experimental tests are conducted for a wide range of working conditions to asses the performance of both technologies under different circumstances and compare the capabilities of these two technologies to boost the performance of transcritical CO_2 vapour compression cycles for low-medium power units.

2. Experimental system

2.1. Refrigeration facility

The low-medium power experimental facility consists of a single stage vapour compression system that is designed to work with CO_2 at transcritical state. It uses a two expansion valve system to control the pressure of the gas-cooler and the useful superheating at the evaporator.

The main elements of the base transcritical refrigeration (Fig. 1 and Fig. 2) system are the following: an hermetic compressor (A), SANDEN SHR17, with a cubic capacity of 1.75cm^3 and a nominal power of 440W while powered at 220V; a coalescent oil filter (B), TECNAC SAC 0-130 bar, that separates up to 98% of the lubricating oil from the compressor; an air finned tube gas-cooler (C), ECO TKE351A2R.1620, provided with a fan that forces air at ambient temperature through its fins; a coriolis flow meter (F), YOKOGAWA ROTAMASS NANO, used to measure the mass flow rate of the CO_2 through the refrigeration facility; a back-pressure electronic valve (G), CAREL E2V05CS100, that maintains the pressure of the gas-cooler at a designated level; an accumulation tank (H), TECNAC RV-10, with a capacity of 10l that connects the 2 electronic valves; a thermostatic electronic valve (I), CAREL E2V05CS100, that is responsible of controlling the useful superheating at the evaporator; a brazed plate evaporator (J), SWEP B18Hx10/1P-SC-U, where the refrigerant evaporates while extracting heat using a secondary fluid; and lastly, an electromagnetic volumetric flowmeter (K), AXG ADMAG TI, that measures the volumetric flow of the secondary fluid. In addition, an auxiliary system is used to force the secondary fluid (water-glycol mixture) through the evaporator. The temperature of the water-glycol mixture (40% glycol) is controlled using a proportionalintegralderivative controller that by the means of an electrical cartridge maintains the evaporation level constant. The system is designed to work under 3 different configurations: base transcritical CO_2 refrigeration cycle (3.a), transcritical CO_2 cycle with IHX (3.b) and transcritical CO_2 cycle with TESC (3.c). A qualitative pressure vs enthalpy diagram is shown for each configuration in Fig. 3.

Fig. 2. Experimental refrigeration facility.

Working under the configuration of the base transcritical CO_2 refrigeration cycle, the compressor increases the pressure and enthalpy of the overheated vapour from point 1 to 2. Then, the fluid is cooled

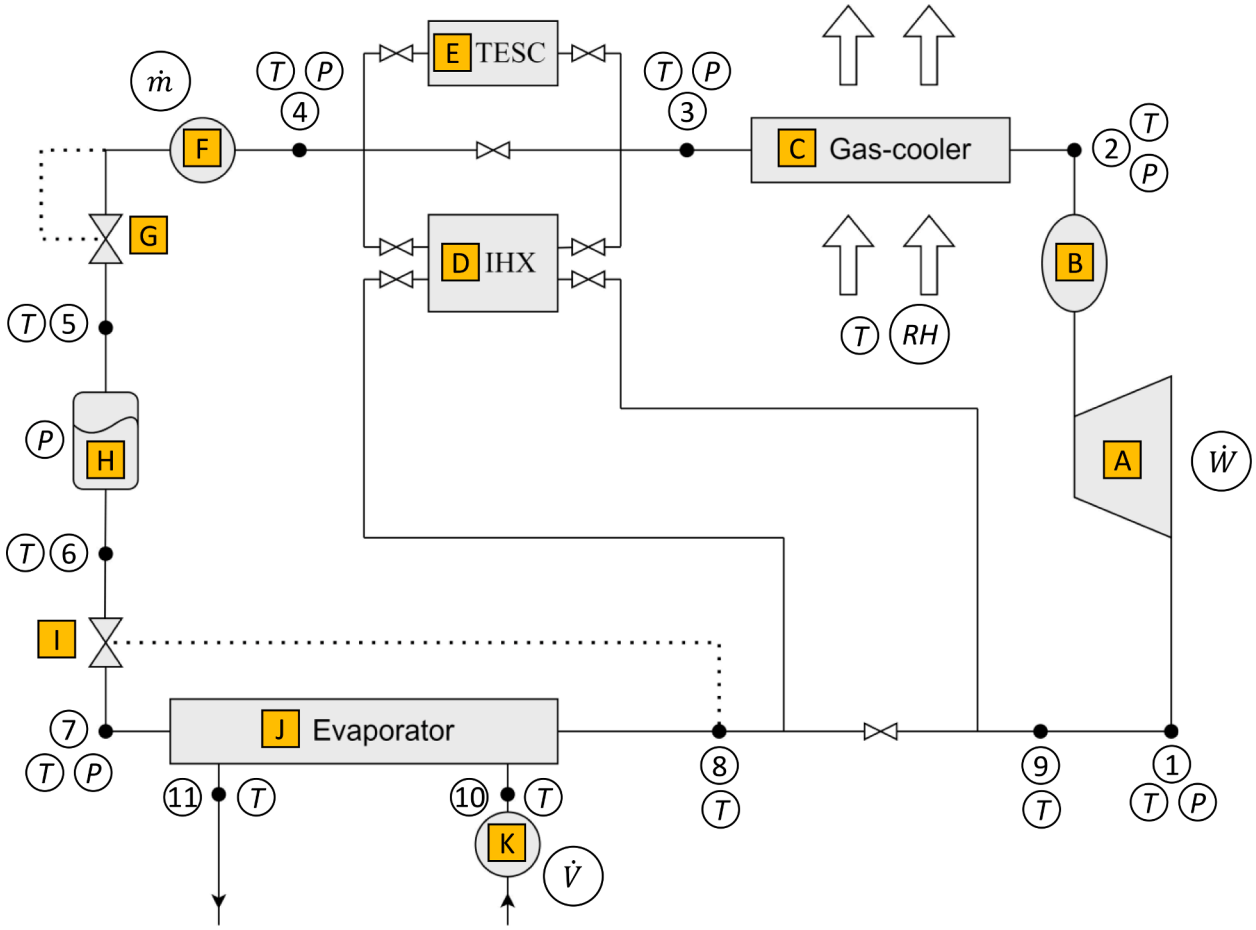

Fig. 1. Schematic of the refrigeration facility with the main elements, measured points and location of the probes.

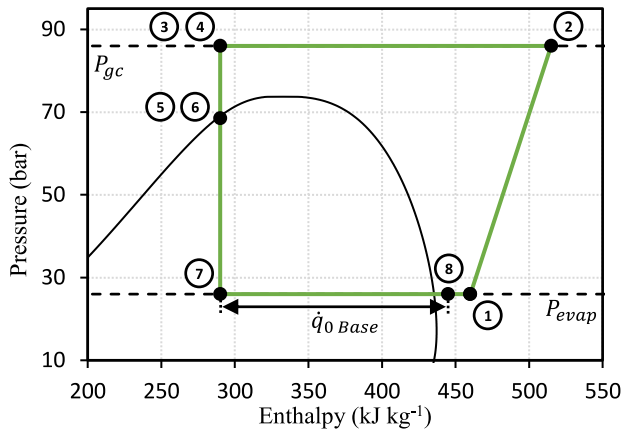

(3.a) P-h diagram of the base transcritical CO_2 cycle

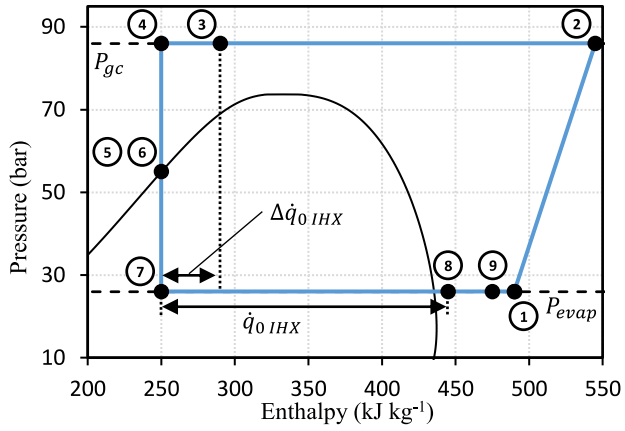

(3.b) P-h diagram of the transcritical CO_2 cycle with IHX

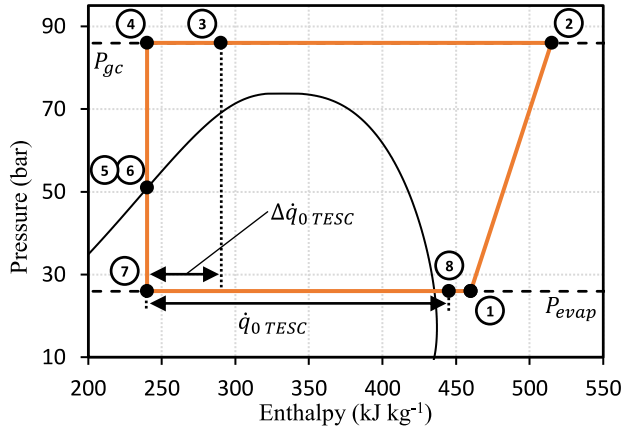

Fig. 3. Pressure vs Enthalpy diagrams for the base transcritical CO_2 cycle (3.a), with the IHX (3.b) and with the TESC (3.c).

down at the gas-cooler releasing heat to the ambient until reaching point 3. Under the base transcritical CO_2 refrigeration cycle configuration, point 3 is bypassed to point 4 and the fluid does not pass through either the IHX or the TESC. Afterwards, the two phase expansion process takes place, the fluid expands in the back-pressure valve and then in the thermostatic valve, from point 4 to 5 and 6 to 7, respectively. Lastly, the fluid absorbs heat at the evaporator from point 7 to 8. In the base cycle configuration, the IHX is not connected and the fluid flows through the bypass from point 8 to 9, closing the thermodynamic cycle.

2.2. Internal heat exchanger (IHX)

The IHX consists of a concentric tube heat exchanger in counterflow configuration (Fig. 4). It is built with stainless steel pipes to support the high pressures of the CO_2. The internal diameter of the inner pipe is 10.4mm with a thickness of 1.7mm and the internal diameter of the outer pipe is 15.8mm with a thickness of 2.8mm. The effective heat exchange length of the heat exchanger is 750mm.

The high pressure fluid at the outlet of the gas-cooler flows through the outer channel while the low pressure vapour at the outlet of the evaporator goes through the inner tube. A natural heat flow appears between the two fluids, subcooling the fluid at the outlet of the gas-cooler from point 3 to 4 and heating the vapour at the outlet of the evaporator from point 8 to 9. The subcooling produced from point 3 to 4 traduces in an increase in the specific cooling capacity at the evaporator. At the same time, it reheats the overheated vapour at the outlet of the evaporator from point 8 to 9, increasing the specific compression work. In a transcritical CO_2 cycle, the improvement obtained at the evaporator compensates the higher specific work at the compressor and as a result, the COP of the refrigeration system is enhanced if properly designed.

2.3. Thermoelectric subcooler (TESC)

The TESC consists of thermoelectric modules (TEMs), heat exchangers for the cold side (in contact with the CO_2) and heat exchangers for the hot side (in contact with the ambient). An schematic of the subcooler with the main elements and the measuring instruments is presented in Fig. 5. The complete subcooler is composed by a total of: 8 heat exchangers for the cold side, 16 TEMs, 16 heat exchangers for the hot side, 4 wind tunnels, 4 low power consumption fans and an electrical power supply to power the TEMs (Fig. 6).

The TESC is subdivided in 4 subcooling blocks and a detailed schematic of one of them is presented in Fig. 7. Each subcooling block is composed by the following elements: 2 heat exchangers for the cold side, where the CO_2 flows and gets subcooled; 4 TEMs, that are responsible of forcing the heat flux between the CO_2 and the ambient; and 4 heat exchangers for the hot side, which release the heat to the ambient.

Each heat exchanger for the cold side consists of a copper block of 56 X 56 X 12mm^3 in which an internal channel for the CO_2 has been mechanized. The inner circuit has a length of 336mm and a circular cross section with a diameter of 3mm that results in an inner heat exchange area of 0.0032m^2. It is provided with 2 planar surfaces of 56 X 56mm^2 where the cold faces of 2 TEMs are placed. The commercial modules used in the TESC are manufactured by Marlow industries and the model reference is RC12-6L. The bismuth-telluride modules are 40 X 40mm^2, present a thickness of 3.9mm and are provided with 127 thermocouples. For the hot side, heat pipe heat exchangers with fins are utilized, the commercial reference of the hot side heat exchanger is Xigmatek HDT-S983 Nepartak. Each of them is provided with 3 heat pipe tubes with a diameter of 8mm and 42 aluminium fins. An expanded drawing of the components is presented in Fig. 8 along the flow of the CO_2 and the energy fluxes. To ensure that a correct heat dissipation takes place in the hot side, an airflow is forced across a wind tunnel

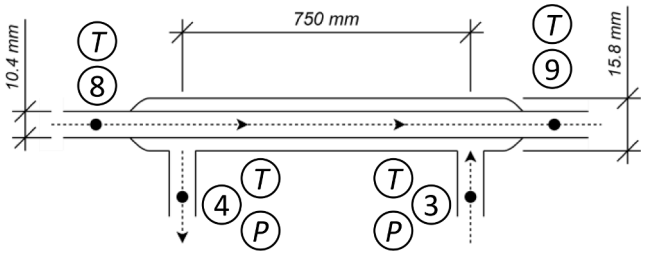

Fig. 4. Schematic of the internal heat exchanger.

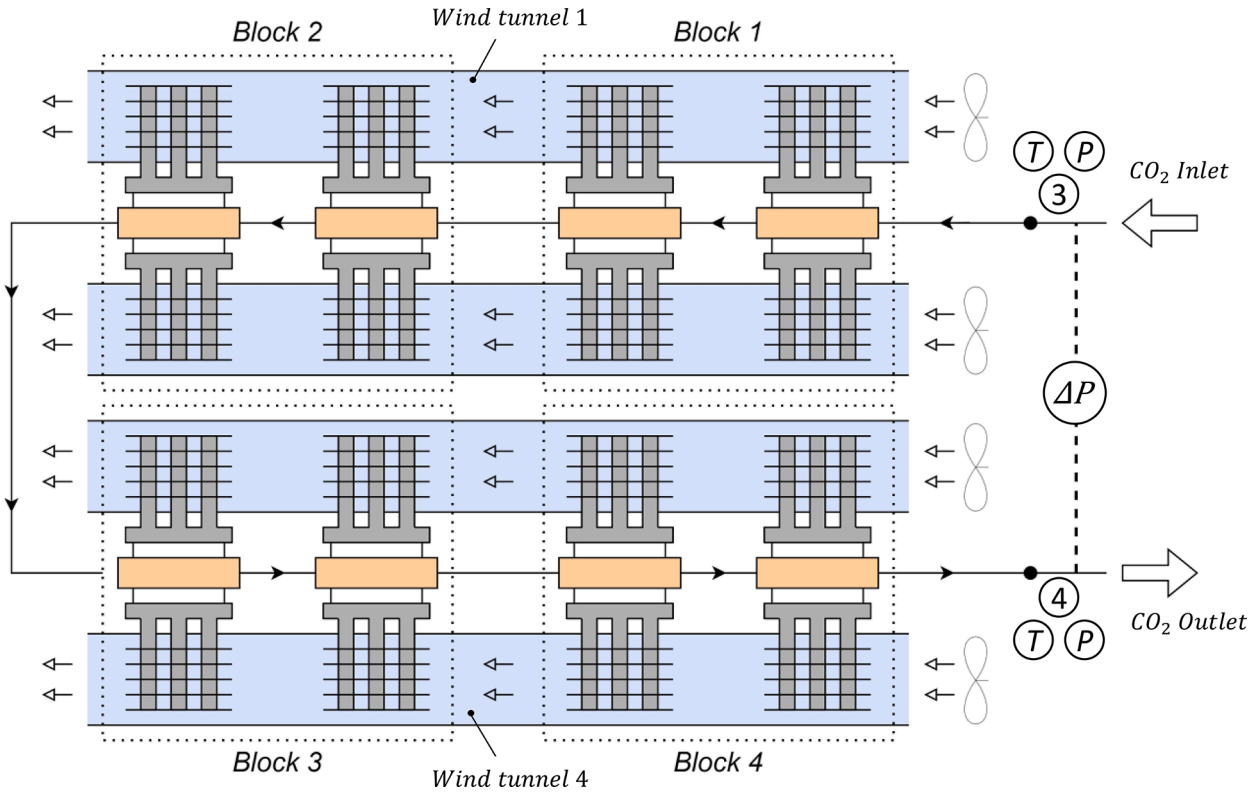

Fig. 5. Schematic of the thermoelectric subcooler (TESC).

Fig. 6. Experimental thermoelectric subcooler.

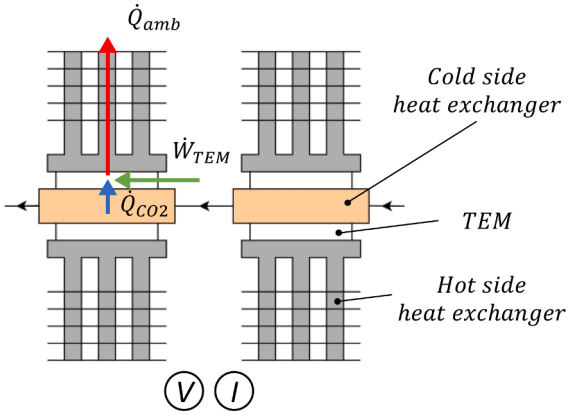

Fig. 7. Detailed schematic of a block of the TESC.

where the fins of 4 heat exchangers of the hot side are located. To fix all the elements together, 8 mm bolts are attached to the hot side heat exchangers which secures the cold side heat exchanger and the TEMs that are placed in the middle of them. Lastly, graphite pads are used as thermal interface materials between the faces of the TEMs and the heat exchangers to reduce the thermal contact resistances.

The TEMs are connected electrically in parallel to an adjustable DC electrical power supply ($\dot{W}_{TEM}$) and by the means of the Peltier effect, a thermal gradient appears between the faces of the TEMs, reducing the temperature of the cold face and rising the temperature of the hot face. The cold face of the TEM is in contact with the heat exchanger of the cold side and the hot face of the TEM is in contact with the hot side heat exchanger. The CO_2 flows through the inner channel of the cold side heat exchanger while heat is extracted from the fluid ($\dot{Q}_{CO2}$), subcooling

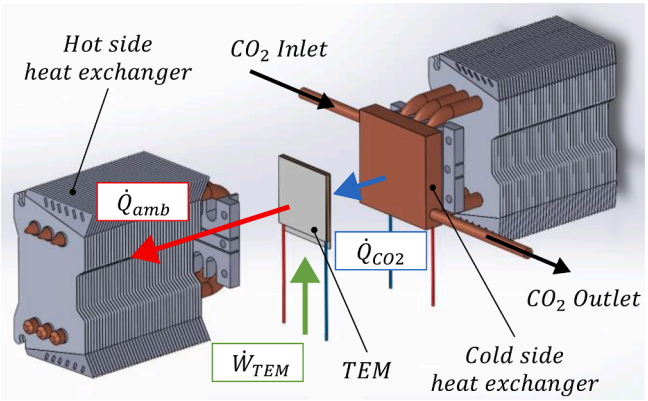

Fig. 8. Expanded view of the subcooling system with energy and heat fluxes.

the refrigerant. The heat passes across the TEM and gets dissipated into the ambient through the heat exchanger of the hot side ($\dot{Q}_{amb}$). The TESC subcools the refrigerant from point 3 to 4 and as a result the specific cooling capacity increases at the evaporator. Also, the power consumption of the whole facility increases as the power consumption of the TEMs is introduced. If properly managed, when the voltage supplied to the TEMs is optimized the increase in cooling capacity compensates the added consumption of the TEMs and as a result the COP of the refrigeration cycle increases.

3. Methodology

3.1. Measuring equipment

The experimental system is completely monitored using measurement probes for: temperature (T), pressure (P), pressure difference (ΔP), relative humidity (RH), power consumption (W), voltage (V), current (I), mass flow rate ($\dot{m}$) and volumetric flow rate ($\dot{V}$).

To measure the temperature of the refrigeration facility T type thermocouples are used. In points 1, 2, 3, 4, 7, 10 and 11, the thermocouples are immersed in the measured fluid and for points 5, 6, 8 and 9 the thermocouples are located in the surface of the pipe. Thermocouples are also used to monitor the faces of the TEMs. In addition, 2 thermoecouples are located to monitor the temperature of the ambient air used to operate the gas-cooler and the TESC. Pressure is collected for 3 different ranges: high pressure gauges are used in points 2, 3 and 4; a medium pressure gauge is used in the tank; and low pressure gauges are utilised for points 7 and 1. A differential pressure sensor is connected between points 3 and 4 to measure the pressure drop at the TESC. An hygrometer is used to measure the relative humidity of the air that flows through the gas-cooler and the TESC. A network analyser is used to collect the power consumption of the compressor. The direct voltage and current supplied to each subcooling block is measured using hall effect sensors and voltmeters. The mass flow rate of the refrigeration facility is measured by a coriolis flow meter, ROTAMASS NANO, located before the back pressure electronic valve. Lastly, the volumetric flow rate of the secondary fluid (water+glycol) is measured using a electromagnetic volumetric meter, AXG ADMAG TI, situated at the inlet of the secondary fluid in point 10. The main characteristics of the measurement equipment is collected in Table 1.

Table 1
Characteristics of the measurement equipment.

Measuring device	Measured variable	Unit	Range	Accuracy
Thermocouple T	Temperature	° C	-35 - 105	±0.5° C
High pressure gauge	Pressure	bar	0 - 160	±0.25% of full scale
Medium pressure gauge	Pressure	bar	0 - 100	±0.25% of full scale
Low pressure gauge	Pressure	bar	0 - 60	±0.25% of full scale
Differential pressure sensor	Pressure difference	bar	0.05 - 5	±0.055% of reading
Hygrometer	Relative humidity	%	0 - 100	±2%
Network analyser	Power consumption	W	0 - 625	±0.5% of reading
Voltmeter	DC voltage	V	0 - 10	±0.5% of reading
Hall effect sensor	DC current	A	0 - 25	±0.2% of reading
Coriolis flow meter	Mass flow rate	kgh^{-1}	0 - 30	±0.2% of reading
Electromagnetic volumetric meter	Volumetric flow rate	$m^3 h^- - 1$	0.002 - 0.2	±0.3% of reading

3.2. Experimental conditions

The evaporation level (T_0) is set to -10° C (commonly used in commercial refrigeration), and the useful superheating at the evaporator (USH) is maintained at 4 K. Also, the volumetric flow rate of the secondary fluid ($\dot{V}_{gly}$) is set to 0.08 m^3/h. Besides, the refrigeration facility is tested inside a climatic chamber, where ambient temperature and relative humidity are controlled.

The tests for the experimental facility are performed for the 3 configurations: base transcritical CO_2 refrigeration cycle (a), transcritical CO_2 cycle with IHX (b) and transcritical CO_2 cycle with TESC (c). The facility is tested under 3 different ambient conditions summarized in Table 2 according to ISO standard ISO 23953-2:2015. Besides, the gas-cooler pressure (P_{gc}) is varied to obtain the optimum working conditions for each configuration of the refrigeration cycle Aprea and Maiorino (2009). Lastly, when the facility is tested with the TESC, the voltage supplied to the TEMs (V_{TEM}) is varied to obtain optimum working conditions of the whole system. During the experimental tests, the facility works until steady state conditions are obtained and afterwards, data is collected for 20 minutes of continuous operation.

The cooling capacity at the evaporator ($\dot{Q}_0$) of the whole refrigeration system is calculated in two ways: using Equation 1 and Equation 2.

$$\dot{Q}_{0\ CO2} = \dot{m}_{CO2} \cdot (h_8 - h_7) \tag{1}$$

$$\dot{Q}_{0\ gly} = \dot{V}_{gly} \cdot \rho_{gly} \cdot c_{p\ gly} \cdot (T_{10} - T_{11}) \tag{2}$$

In Eq. 1 the cooling capacity is obtained with data collected with the refrigeration cycle ($\dot{Q}_{0\ CO2}$) and in Eq. 2 the value is obtained through data from the auxiliary system ($\dot{Q}_{0\ gly}$). Both data are compared and represented in Fig. 9 for all the experimental tests. The comparative shows a great agreement of the data, with all deviations between the ±5% interval. This good agreement proves the reliability and consistency of the experimental methodology employed during the tests.

4. Results and discussion

4.1. Base transcritical carbon dioxide cycle

The COP is obtained as in Eq. 3 for the base transcritical refrigeration cycle, where the cooling capacity is calculated with the data collected from the auxiliary system as in Eq. 2. In Fig. 10 the COP of the base transcritical cycle is presented as a function of the pressure of the gas-cooler for the 3 different ambient conditions. The optimum COP obtained for the base transcritical cycle was 1.85 for climatic class 3, 1.48 for climatic class 4 and 1.14 for climatic class 7. Regarding the cooling capacity, 713.7, 600.2 and 504.5W were obtained for climatic class conditions 3, 4 and 7, respectively. More relevant data for the base cycle optimum points is collected in Table 3.

$$COP_{base} = \frac{\dot{Q}_0}{\dot{W}_{tot}} = \frac{\dot{Q}_{0\ base}}{\dot{W}_{comp}} \tag{3}$$

The results obtained for the base transcritical cycle remark the impact that ambient conditions have on the performance of the CO_2 vapour compression cycle. When ambient temperature raises from 25 to 35° C, the COP of the refrigeration cycle decreases drastically, from 1.85 to 1.14, a 34.8% decrease in the performance. In addition the cooling capacity also drops, from 713.7 to 504.5W, which translates in a 29.3%

Table 2
Climatic class conditions (ISO 23953-2:2015 at $T_0 = -10°C$).

Climatic class	T_{amb} (° C)	RH_{amb} (%)
3	25	60
4	30	55
7	35	75

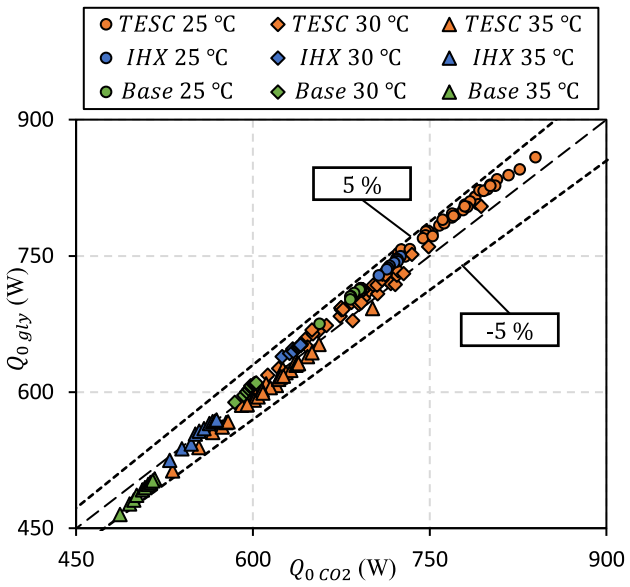

Fig. 9. Comparative for the cooling capacity of the refrigeration facility between experimental data from the transcritical CO_2 cycle and experimental data from the auxiliary system.

decrease in the cooling power of the installation. Regarding the design of refrigeration facilities, the decrease in cooling capacity is extremely relevant, as facilities need to have enough cooling capacity for the hottest days of the year and therefore, need to be designed accordingly.

4.2. Transcritical cycle with internal heat exchanger (IHX)

The inclusion of an internal heat exchanger, being a passive system, does not add any extra consumption. Thus, the COP of the transcritical cycle with IHX is calculated in the same way as in the base cycle, using Eq. 4. The results for the optimum operation conditions with the IHX, are collected in Table 4 for each climatic class. The percentage variations for the COP and the cooling power are calculated in comparison with the base cycle values at the same climatic class conditions using Eq. 5 where X is either the COP or the cooling power.

$$COP_{IHX} = \frac{\dot{Q}_0}{\dot{W}_{tot}} = \frac{\dot{Q}_{0\ IHX}}{\dot{W}_{comp}} \tag{4}$$

$$\Delta X = \frac{X - X_{base}}{X_{base}} \cdot 100 \tag{5}$$

The IHX boosts the performance of the transcritical CO_2 cycle. For climatic class 3, the improvements in comparison with the base cycle are 6.8% in the COP and 4.9% in cooling capacity. As temperature increases, the performance of the base cycle goes down, hence, the enhancements obtained with the IHX are greater. For climatic class 4, the COP increases 8.5% and the enhancement in cooling capacity is 7.1%. Lastly, for climatic class 7 the enhancement in COP is 13.6% and the improvement in cooling capacity is 10.4%. In addition, the inclusion of the IHX also affects the optimum gas-cooler pressure of the cycle. Although in climatic class 3 the optimum pressure remains very similar, for climatic class 4 and 7 the optimum pressure drops 1 and 2bar, respectively. Also, the discharge temperature increases 7.3-8.6° C in comparison with the base cycle due to the higher suction temperatures. Lastly, it is important to highlight the reduction of the mass flow rate of CO_2 obtained with the IHX that is produced due to the increase of the temperature at the suction line of the compressor in comparison with the base cycle.

Summarizing, the inclusion of an IHX presents itself as a simple passive solution to boost the performance of the base transcritical cycle. The results show that general improvements in the COP and the cooling

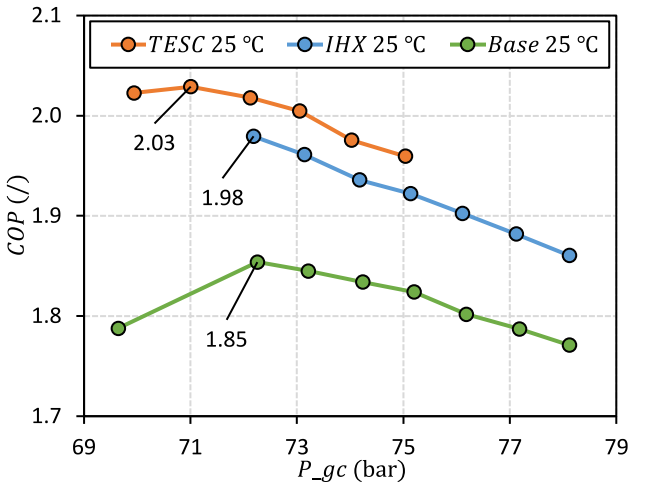

(10.a) COP vs P_{gc} for class 3 (T_{amb} = 25 °C and HR_{amb} = 60 %)

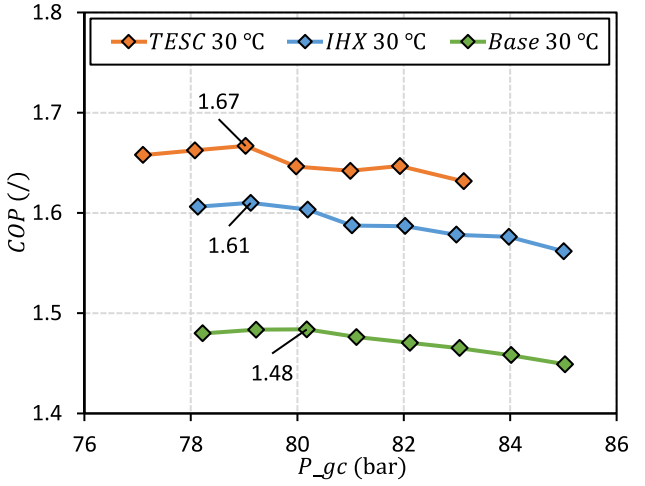

(10.b) COP vs P_{gc} for class 4 (T_{amb} = 30 °C and HR_{amb} = 55 %)

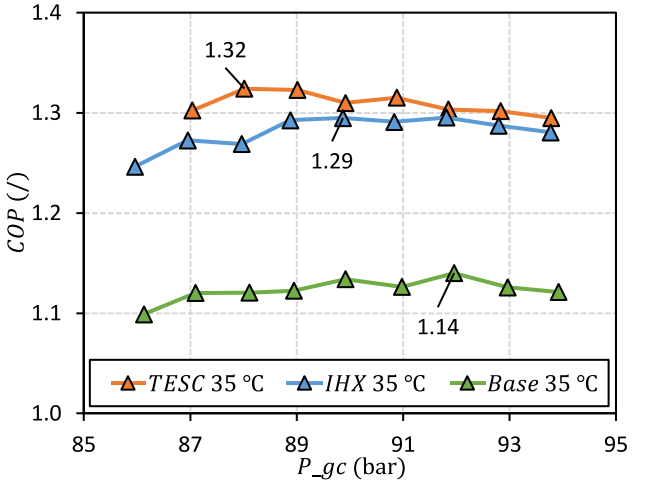

(10.c) COP vs P_{gc} for class 7 (T_{amb} = 35 °C and HR_{amb} = 75 %)

Fig. 10. COP vs P_{gc} for the base transcritical CO_2 cycle, transcritical cycle with IHX and transcritical cycle with TESC for 3 climatic class conditions: climatic class 3 (10.a), climatic class 4 (10.b), and climatic class 7 (10.c).

Table 3
Results for base cycle at optimum operation conditions for climatic class conditions 3, 4 and 7.

Climatic class	$P_{gc\ opt}$ (bar)	T_{dis} (° C)	$\dot{m}_{CO2}$ (kgh^{-1})	$\dot{W}_{comp}$ (W)	COP_{base}	$\dot{Q}_{0\ base}$ (W)
3	72.3	81.7	14.90	385.0	1.85	713.7
4	80.2	91.1	14.22	404.5	1.48	600.2
7	91.9	104.7	13.42	442.6	1.14	504.5

capacity of the refrigeration system were achieved while slightly decreasing the optimum gas-cooler pressure of the refrigeration facility for al climatic class conditions tested.

4.3. Transcritical cycle with thermoelectric subcooler (TESC)

With the inclusion of the TESC, the voltage supplied to the TEMS (V_{TEMs}) is another important variable that is added for the operation of the cycle. For each gas-cooler pressure tested, the voltage supplied to the TEMs is varied from 0.5 to 6 V. To calculate the COP of the transcritical cycle with TESC, Eq. 6 is used. The COP of the transcritical cycle with TESC is presented as a function of the pressure of the gas-cooler in Fig. 10. The COP is calculated as in Eq. 6 by adding the power consumption of the TEMs of the subcooler to Eq. 5. For each pressure, each represented point corresponds to the optimum voltage supplied to the TEMs that maximizes the COP of the whole refrigeration system. In addition, Table 4 collects the main results for optimum operation conditions with the TESC.

The result of including the TESC is proven beneficial for all the climatic classes conditions tested. For climatic class 3, an optimum COP of 2.03 is obtained with a voltage supplied to the TEMs of 2.0V and a gas-cooler pressure of 71.0bar. The percentage improvement in the COP is 9.4% while also increasing the cooling capacity a 14.1% in comparison with the base cycle. As ambient temperature increases, the improvements obtained with the TESC are more noticeable. For climatic class 4, at an ambient temperature of 30° C, the improvement in the COP is 12.3% and the cooling capacity is enhanced a 17.8%. Lastly, for climatic class 7 at an ambient temperature of 35° C, the COP improves 16.2% and the cooling capacity is enhanced 20.8%.

$$COP_{TESC} = \frac{\dot{Q}_0}{\dot{W}_{tot}} = \frac{\dot{Q}_{0\ TESC}}{\dot{W}_{comp} + \dot{W}_{TEMs}} \tag{6}$$

The optimum pressure of the gas-cooler also drops when including the TESC. For climatic class conditions 3, 4 and 7, a decrease of 1.3, 1.2 and 3.9bar, respectively, is registered during the experimental tests. The direct effect of the reduction of the pressure is a decrease in the compression ratio that improves the performance of the compressor as well as a slight decrease of 0.1-2.8° C in the discharge temperature of the compressor. Hence, an increase in mass flow rate of the refrigerant is registered in comparison with the base cycle: from 14.90 to 15.15kgh^{-1} in climatic class 3 conditions, from 14.22 to 14.38kgh^{-1} in climatic class 4 conditions and lastly from 13.42 to 13.62kgh^{-1} in climatic class 7 conditions. The maximum pressure drop registered with the differential pressure sensor at the subcooler is 420mbar. This low pressure drop is virtually negligible in comparison with the pressure levels at the gas-cooler and therefore, does not negatively affect the vapour compression system.

The effect of the voltage supplied to the TEMs of the TESC is also analysed in Fig. 11. When the voltage supplied to the TEMs is small, the cooling capacity increases slowly while the increment in power consumption is low. For high voltages, the increase in cooling capacity is very noticeable but the power consumption rises drastically, resulting in a lower COP of the refrigeration facility. An optimum value of 2.03 is obtained for the COP at a voltage supplied to the TEMs of 2V, where the increase in cooling capacity is noticeable (14.1%) and the increment in power consumption due to the TEMs in comparison with the base cycle is low (4.3%), resulting in an enhancement of the COP of 9.4% at climatic class 3 conditions.

Moreover, graph 11.b of Fig. 11 shows the COP of the TEMs and the COP of the cycle as a function of the voltage supplied to the TEMS. The COP of the TEMs is defined as the coefficient of performance of the modules of the TESC and is obtained through Eq. 7. Graph 10.b shows clearly that for low voltages supplied to the TEMs the COP of the TEMs is very high while producing very little subcooling, when the voltage is increased, the subcooling responds linearly while reducing the COP of the TEMs exponentially. This linear subcooling as a function of the voltage supplied to the TEMs remarks the simplicity of the control system needed for the TESC. It is also important to note that, for climatic class 7 conditions, when the COP of the base cycle is low, the optimum voltage supplied to the TEMs rises to 2,5 V. Lastly, Table 5 shows the subcooling produced in each block of the TESC for the optimum operation conditions at each climatic class. It clearly shows that the optimum value for the total subcooling is similar in all cases between 5.3-6.1° C and that the subcooling produced in each block for optimum operation conditions varies between 1.2-1.8° C, which is affected by the ambient conditions or the voltage supplied to the TEMs.

$$COP_{TEM} = \frac{\dot{Q}_{TEMs}}{\dot{W}_{TEMs}} \tag{7}$$

In summary, the inclusion of the TESC improves significantly the COP and the cooling capacity of the facility for all climatic class conditions tested. Besides, a small decrease in the optimum gas-cooler pressure is obtained during the experimental tests. Lastly, the subcooling produced can be approximated to a linear function of the voltage supplied to the modules, which translates into a simple control of the whole vapour compression system.

4.4. Evaluation of the IHX and the TESC

Both the IHX and the TESC studied in this work enhance the performance of the base transcritical CO_2 cycle for climatic class conditions 3, 4 and 7. In addition, a slight decrease in gas-cooler pressure is reported for both technologies. The IHX presents itself as a simple, passive solution that boosts the performance of the system. The TESC, although it consists of more elements than the IHX, is an scalable controllable simple solution that obtains greater improvements in the COP and cooling capacity in comparison with the IHX.

Regarding the COP, the enhancements obtained with the TESC

Table 4
Results for transcritical cycle with IHX and with TESC at optimum operation conditions for climatic class conditions 3, 4 and 7.

Climatic class	Cycle configuration	$P_{gc\ opt}$ (bar)	$\Delta P_{gc\ opt}$ (bar)	T_{dis} (° C)	$\dot{m}_{CO2}$ (kgh^{-1})	Sub (K)	$\dot{W}_{comp}$ (W)	V_{TEM} (V)	$\dot{W}_{TEMs}$ (W)	$\dot{W}_{tot}$ (W)	COP (/)	ΔCOP (%)	$\dot{Q}_0$ (W)	$\Delta\dot{Q}_0$ (%)
3	IHX	72.2	- 0.1	89.7	14.06	4.7	378.2	-	-	378.2	1.98	+ 6.8	748.6	+ 4.9
	TESC	71.0	- 1.3	80.9	15.15	6.1	379.1	2.0	22.4	401.5	2.03	+ 9.4	814.5	+ 14.1
4	IHX	79.2	- 1.0	99.7	13.38	4.4	399.1	-	-	399.1	1.61	+ 8.5	642.5	+ 7.1
	TESC	79.0	- 1.2	91.0	14.38	5.3	402.4	2.0	21.8	424.2	1.67	+ 12.3	707.1	+ 17.8
7	IHX	89.9	- 2.0	112.0	12.54	5.1	430.2	-	-	430.2	1.29	+ 13.6	557.0	+ 10.4
	TESC	88.0	- 3.9	101.9	13.62	6.0	426.7	2.5	33.3	460.0	1.32	+ 16.2	609.2	+ 20.8

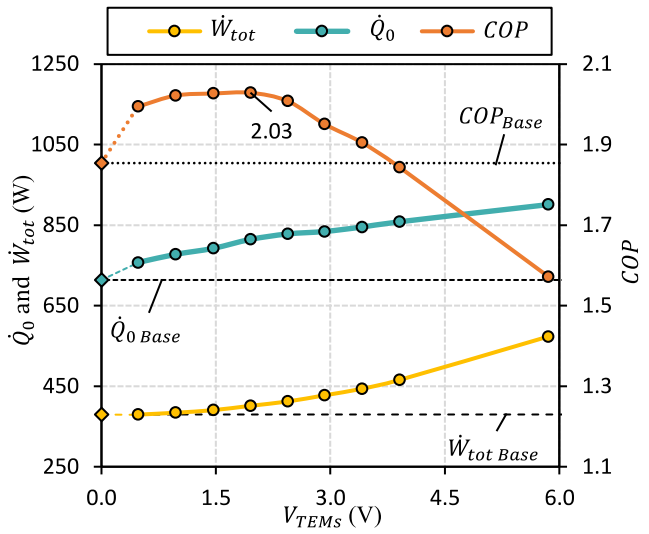

(11.a) $\dot{Q}_0$, $\dot{W}_{tot}$ and COP vs V_{TEMs}

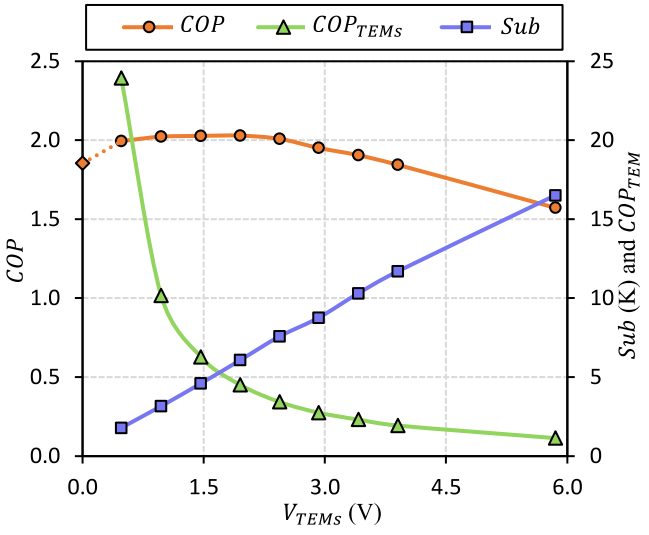

(11.b) COP, COP_{TEMs} and Sub vs V_{TEMs}

Fig. 11. Analysis of the effect of the voltage supplied to the TEMs on the transcritical cycle with TESC for climatic class 3 optimum working conditions

Table 5
Subcooling in each block of the TESC at optimum operation conditions for climatic class conditions 3, 4 and 7.

Climatic class	V_{TEM} (V)	Sub (K)	Sub_1 (K)	Sub_2 (K)	Sub_3 (K)	Sub_4 (K)
3	2.0	6.1	1.6	1.4	1.5	1.6
4	2.0	5.3	1.3	1.2	1.3	1.5
7	2.5	6.0	1.3	1.3	1.6	1.8

outperform the ones obtained with the IHX for all climatic class conditions tested, as Table 4 shows. Also, the enhancements in the cooling capacity are also greater when using the TESC and the decrease in gas-cooler pressure, although low in both cases, are higher for the TESC.

Moreover, the TESC allows a control of the subcooling of the installation which is directly proportional to the voltage supplied to the TEMs. When the TESC is supplied with high voltages, the increase in cooling capacity is very noticeable, at climatic class 3 conditions, when supplied with 6 V the coooling capacity of the refrigeration facility is boosted to 901.2W, that compared with the 713.7W of the base transcritical cycle, results in a 26.3% increase in the cooling capacity. This feature of the TESC allows for more flexible design of refrigeration facilities. As an example, for the hottest days of the year, a refrigeration facility with a TESC could work with high voltages for the TEMs, resulting in lower COPs and a big cooling capacity that would be able to supply the cooling demand of these hot days. In that way, the refrigeration facility would not need to be so oversized and therefore, a smaller facility that on the hottest days uses the TESC at full power, would be able to meet the cooling demands over the year.

5. Conclusions

This work presents an experimental study in which a low-medium power transcritical CO_2 refrigeration facility has been tested under base transcritical cycle, with an internal heat exchanger and with a thermoelectric subcooler.

Both the technologies studied in this work present themselves as remarkable solutions for improving the performance of transcritical CO_2 cycles. The internal heat exchanger, being a passive system, highlights due to its simplicity of installation and operation. The thermoelectric subcooler stands out due to its scalability, flexibility, easy control, and greater enhancements reported in both coefficient of performance and cooling capacity. The experimental system is tested for 3 different ambient conditions and the optimum gas-cooler pressure is obtained for each configuration.

1. The internal heat exchanger enhanced the coefficient of performance of the cycle 6.8%, 8.5% and 13.3% for climatic class conditions 3, 4 and 7, respectively.
2. The internal heat exchanger reported improvements in the cooling capacity of 4.9%, 7.1% and 10.4% for climatic class conditions 3, 4 and 7, respectively.
3. The thermoelectric subcooler outperformed the internal heat exchanger in coefficient of performance by reported enhancements on the coefficient of performance of the cycle of 9.4%, 12.3% and 16.2% for climatic class conditions 3, 4 and 7, respectively.
4. The thermoelectric subcooler also reported even greater improvements than the internal heat exchanger in cooling capacity of 14.1%, 17.8% and 20.8% for climatic class conditions 3, 4 and 7, respectively.

Lastly, the thermoelectric subcooler allows a simple control of the subcooling that is directly proportional to the voltage supplied to the thermoelectric modules. This feature would allow smaller facilities with a thermoelectric subcooler to meet greater cooling demands during short periods of time and therefore, avoid an excessive oversize of the refrigeration facility.

Declaration of Competing Interest

The authors declare that they have no known competing financial interests or personal relationships that could have appeared to influence the work reported in this paper.

Acknowledgements

The authors would like to acknowledge the support of the Spanish Ministry of Science, Innovation and Universities, and European Regional Development Fund, for the funding under the RTI2018-093501-B-C21 and RTI2018-093501-B-C22 research projects. We would also like to acknowledge the support from the Education Department of the Government of Navarra with the *Predoctoral Grants for Phd programms of Interest to Navarra* and the Official School of Industrial Engineers of Navarre with the scholarship *Fuentes Dutor*. Open access funding provided by Universidad Pública de Navarra.

References

Aprea, C., Maiorino, A., 2008. An experimental evaluation of the transcritical co2 refrigerator performances using an internal heat exchanger. International Journal of Refrigeration 31, 1006–1011. https://doi.org/10.1016/j.ijrefrig.2007.12.016.

Aprea, C., Maiorino, A., 2009. Heat rejection pressure optimization for a carbon dioxide split system: An experimental study. Applied Energy 86, 2373–2380. https://doi.org/10.1016/j.apenergy.2009.03.006.

Aranguren, P., Sánchez, D., Casi, A., Cabello, R., Astrain, D., 2021. Experimental assessment of a thermoelectric subcooler included in a transcritical co2 refrigeration plant. Applied Thermal Engineering 190. https://doi.org/10.1016/j.applthermaleng.2021.116826.

Catalán-Gil, J., Nebot-Andrés, L., Sánchez, D., Llopis, R., Cabello, R., Calleja-Anta, D., 2020. Improvements in co2 booster architectures with different economizer arrangements. Energies 13. https://doi.org/10.3390/en13051271.

Cecchinato, L., Chiarello, M., Corradi, M., 2010. Design and experimental analysis of a carbon dioxide transcritical chiller for commercial refrigeration. Applied Energy 87, 2095–2101. https://doi.org/10.1016/j.apenergy.2009.12.009.

Chesi, A., Esposito, F., Ferrara, G., Ferrari, L., 2014. Experimental analysis of r744 parallel compression cycle. Applied Energy 135, 274–285. https://doi.org/10.1016/j.apenergy.2014.08.087.

Dai, B., Cao, Y., Liu, S., Ji, Y., Sun, Z., Xu, T., Zhang, P., Nian, V., 2022. Annual energetic evaluation of multi-stage dedicated mechanical subcooling carbon dioxide supermarket refrigeration system in different climate regions of china using genetic algorithm. Journal of Cleaner Production 333. https://doi.org/10.1016/j.jclepro.2021.130119.

IIR, 2017. 35th informatory note on refrigeration technologies / the impact of the refrigeration sector on climate change.

IIR, 2019. 38th informatory note on refrigeration technologies / the role of refrigeration in the global economy.

Kim, M.H., Pettersen, J., Bullard, C.W., 2004. Fundamental process and system design issues in co2 vapor compression systems. Progress in Energy and Combustion Science 30, 119–174. https://doi.org/10.1016/j.pecs.2003.09.002.

Liu, F., Groll, E.A., Li, D., 2012. Investigation on performance of variable geometry ejectors for co2 refrigeration cycles. Energy 45, 829–839. https://doi.org/10.1016/j.energy.2012.07.008.

Llopis, R., Sánchez, D., Sanz-Kock, C., Cabello, R., Torrella, E., 2015. Energy and environmental comparison of two-stage solutions for commercial refrigeration at low temperature: Fluids and systems. Applied Energy 138, 133–142. https://doi.org/10.1016/j.apenergy.2014.10.069.

Nebot-Andrés, L., Catalán-Gil, J., Sánchez, D., Calleja-Anta, D., Cabello, R., Llopis, R., 2020. Experimental determination of the optimum working conditions of a transcritical co2 refrigeration plant with integrated mechanical subcooling. International Journal of Refrigeration 113, 266–275. https://doi.org/10.1016/j.ijrefrig.2020.02.012.

Robinson, D. M., Groll, E. A., 1998. Efficiencies of transcritical co 2 cycles with and without an expansion turbine.

Sánchez, D., Aranguren, P., Casi, A., Llopis, R., Cabello, R., Astrain, D., 2020. Experimental enhancement of a co2 transcritical refrigerating plant including thermoelectric subcooling. International Journal of Refrigeration 120, 178–187. https://doi.org/10.1016/j.ijrefrig.2020.08.031.

Sarkar, J., Agrawal, N., 2010. Performance optimization of transcritical co2 cycle with parallel compression economization. International Journal of Thermal Sciences 49, 838–843. https://doi.org/10.1016/j.ijthermalsci.2009.12.001.

Schoenfeld, J., Muehlbauer, J., Hwang, Y., Radermacher, R., orderlihtml Schoenfeld, 2008. Integration of a thermoelectric subcooler into a carbon dioxide transcritical vapor compression cycle refrigeration system. http://docs.lib.purdue.edu/iracc/903.

Sharma, S., Dwivedi, V.K., Pandit, S.N., 2014. A review of thermoelectric devices for cooling applications. International Journal of Green Energy 11, 899–909. https://doi.org/10.1080/15435075.2013.829778.

Shecco, 2016. F-gas regulation shaking up the hvac and r industry.

Torrella, E., Sánchez, D., Llopis, R., Cabello, R., 2011. Energetic evaluation of an internal heat exchanger in a co2 transcritical refrigeration plant using experimental data. International Journal of Refrigeration 34, 40–49. https://doi.org/10.1016/j.ijrefrig.2010.07.006.

Zhu, Y., Li, C., Zhang, F., Jiang, P.X., 2017. Comprehensive experimental study on a transcritical co2 ejector-expansion refrigeration system. Energy Conversion and Management 151, 98–106. https://doi.org/10.1016/j.enconman.2017.08.061.